scientific reports

Check for updates

OPEN

Liver-specific Coxsackievirus and adenovirus receptor deletion develop metabolic dysfunction–associated fatty liver disease

Hong-Gi Kim[1,5], Jin-Ho Park[1,5], Ha-Hyun Shin[1,5], So-Hee Kim[1], Ha-Eun Jeon[1], Ji-Hwa Shin[1], Young-Suk Won[3], Hyo-Jung Kwon[4], Eun-Seok Jeon[2] & Byung-Kwan Lim[1]✉

Metabolic dysfunction–associated fatty liver disease (MAFLD) is a common liver disease associated with obesity and is caused by the accumulation of ectopic fat without alcohol consumption. Coxsackievirus and adenovirus receptor (CAR) are vital for cardiac myocyte-intercalated discs and endothelial cell-to-cell tight junctions. CAR has also been reported to be associated with obesity and high blood pressure. However, its function in the liver is still not well understood. The liver of obese mice exhibit elevated CAR mRNA and protein levels. Furthermore, in the liver of patients with non-alcoholic steatohepatitis, CAR is reduced in hepatocyte cell–cell junctions compared to normal levels. We generated liver-specific CAR knockout (KO) mice to investigate the role of CAR in the liver. Body and liver weights were not different between wild-type (WT) and KO mice fed a paired or high-fat diet (HFD). However, HFD induced significant liver damage and lipid accumulation in CAR KO mice compared with WT mice. Additionally, inflammatory cytokines transcription, hepatic permeability, and macrophage recruitment considerably increased in CAR KO mice. We identified a new interaction partner of CAR using a protein pull-down assay and mass spectrometry. Apolipoprotein B mRNA editing enzyme catalytic polypeptide-like 3C (APOBEC3C) demonstrated a complex relationship with CAR, and hepatic CAR expression tightly regulated its level. Moreover, Apolipoprotein B (ApoB) and Low-density lipoprotein receptor (LDLR) levels correlated with APOBEC3C expression in the liver of CAR KO mice, suggesting that CAR may regulate lipid accumulation by controlling APOBEC3C activity. In this study, we showed that hepatic CAR deficiency increased cell-to-cell permeability. In addition, CAR deletion significantly increased hepatic lipid accumulation by inducing ApoB and LDLR expression. Although the underlying mechanism is unclear, CARs may be a target for the development of novel therapies for MAFLD.

Keywords Coxsackievirus and adenovirus receptor, APOBEC3C, Apolipoprotein B, Paracellular permeability, Metabolic dysfunction–associated fatty liver disease

Metabolic dysfunction–associated fatty liver disease (MAFLD) has become the most common liver disease worldwide in recent years, and its incidence is increasing with the increasing obese population. MAFLD is a disease in which ectopic fat accumulates in the liver in the absence of alcohol consumption. Fatty liver can progress from steatosis, which is fat accumulation without inflammation, to non-alcoholic steatohepatitis (NASH) with fibrosis or severe hepatocellular carcinoma[1–3]. In the development and progression of MAFLD, excessive production of inflammatory cytokines by hepatocyte stimulation due to oxidative stress plays an important role in steatosis

[1]Department of Biomedical Science, Jungwon University, 85 Munmu-ro, Goesan-eup, Goesan-gun, Chungbuk 367-700, Korea. [2]Division of Cardiology, Samsung Medical Center, Sungkyunkwan University School of Medicine, 50 Irwon Dong, Gangnam-Gu, Seoul 06351, Korea. [3]Laboratory Animal Resource Center, Korea Research Institute of Bioscience and Biotechnology, Chungbuk, Korea. [4]Department of Veterinary Pathology, College of Veterinary Medicine, Chungnam National University, Daejeon, Korea. [5]These authors contributed equally: Hong Gi Kim, Jin Ho Park and Ha Hyun Shin. ✉email: bklim@jwu.ac.kr

due to fat accumulation in hepatocytes[4,5]. When a fatty liver develops, adipocytes accumulate and increase triglycerides (TGs) in the liver, blood secretion dysfunction occurs after the synthesis of lipoproteins, and fat from peripheral adipose tissue is transported to the liver. In addition, MAFLD is associated with tight junction (TJ) integrity. In the liver, TJ proteins have several functions: they control paracellular diffusion between adherent hepatocytes and the blood-biliary barrier. TJ proteins maintain intracellular communication and the assembly of signaling proteins, growth factors, cytokines, and signaling cascades to induce and regulate their localization and expression, which contributes to fat accumulation in hepatocytes[6,7]. PECAM-1-deficient mouse develops progressive nonalcoholic fatty liver disease (NAFLD), supporting a role for PECAM-1 as a negative regulator of NAFLD progression[8]. However, the mechanism of MAFLD remains unclear.

Coxsackievirus and adenovirus receptor (CAR) is a membrane protein of 46 kDa that is widely known as a receptor for coxsackievirus type B3. CARs are located in the intercalated discs of cardiomyocytes or TJs of epithelial and endothelial cells. It plays an important role in the cytoskeleton and paracellular interaction[9–12]. CAR containing intra- and extracellular domains is known to interact with the TJ protein ZO-1 and regulates TJ formation and paracellular permeability in epithelial cells[13,14]. It is also involved in maintaining the cytoskeleton along with fibronectin, microtubules, and actin. In particular, CARs can enhance inflammatory interactions between immune and muscle cells in cell–cell communication and regulate the activation of cytokine signaling pathways in the immune system[15–17].

MAFLDs differ according to race and catch up with Western prevalence in Asian urbanized lifestyles. In an African American study, CAR was identified as a gene that affects blood pressure and obesity[18]. In addition, human liver biopsy analysis according to the NASH progression stage showed low levels of CAR expression in patients with obesity and MAFLD[19]. The importance of CAR in cardiovascular diseases and endothelial and epithelial cells is well-known[9,20–23]. However, little is known about the role of CAR in the liver. In particular, the paracellular permeability of fat and TJ protein expression was not associated with MAFLD progression.

This study aimed to investigate the relationship between CAR and MAFLD to demonstrate the role of CAR in lipid accumulation in the mouse liver. It also plays an important role in liver lipid metabolism by identifying new interaction partners of CAR. In this study, we demonstrated that CAR expression was significantly diminished in liver specimens of patients with NASH compared to normal patients. CAR knockout mice developed MAFLD after 16 weeks of high-fat diet (HFD) feeding. Lipid uptake and inflammatory cell infiltration significantly increased. Moreover, we identified a novel interaction partner of CAR, Apolipoprotein B mRNA editing enzyme catalytic polypeptide-like 3C (APOBEC3C)[24–26], which regulates ApoB formation and lipoprotein transport to the liver. It is initially discovered as an antiviral effector of retrovirus (HIV-1) through mRNA modification[25,27]. These findings suggest that the CAR can be a potential therapeutic target for MAFLD.

Results

CAR is downregulated in obese mice and livers of patients with NASH

CAR mRNA and protein expression in the livers of obese mice were observed using RT-PCR and western blot analysis, respectively. C57BL/6 mice were fed an HFD containing 42% fat and 0.2% cholesterol for 16 weeks. Liver RNA was isolated from obese mice, and CAR transcription was analyzed using qPCR. CAR mRNA expression was significantly reduced in the livers of obese mice by approximately 75% compared to that in normal chow-fed mice (**$P < 0.01$) (Fig. 1A). Moreover, CAR protein expression was significantly reduced in the liver of obese mice by approximately 25% ($P < 0.05$). When obesity was induced, C57BL/6 mice showed decreased CAR expression in the liver (Fig. 1B). Furthermore, we observed CAR expression in patients with liver disease. Liver tissue specimens from patients with NASH were purchased from the company and then subjected to multi-dot immunohistochemistry using an anti-CAR antibody. The results showed that CAR was decreased in the cell–cell junctions of hepatocytes of patients with NASH compared to that in liver samples from normal patients (Fig. 1C, Supplement Fig. S1). These results suggested that CAR expression is associated with lipid accumulation the liver.

CAR interacts with APOBEC3C

Next, we sought to identify an interaction partner for the CARs related to changes in hepatocyte permeability and lipid inflow. A FLAG-tagged CAR plasmid was overexpressed in HEK293 cells, and pull-down experiments were performed using FLAG-agarose beads. A new protein expressed only in the CAR overexpression group compared to the control group was extracted and analyzed by mass spectrometry (Supplement Table S2). Therefore, APOBEC3C was selected from several proteins interacting with CAR (Fig. 2A). To confirm whether it directly or indirectly interacted with human CAR, we cloned the human APOBEC3C gene into the pEGFP-C3 plasmid. After HEK293 cells were co-transfected with FLAG-CAR and either GFP-APOBEC3C or GFP, co-immunoprecipitation was performed using anti-FLAG-agarose beads. Western blotting was performed to detect CAR bound to APOBEC3C through GFP detection, and a protein interaction between CAR and APOBEC3C was observed (Fig. 2B). The opposite-direction experiment showed the same results. Overexpression of Flag-APOBEC3C also pulled down the intracellular endogenous CAR protein (Fig. 2C). These results demonstrate that CAR can form complexes with the subcellular modulator protein APOBEC3C. Surprisingly, APOBEC3C, which interacts with CAR, edits ApoB mRNA and induces the early termination of ApoB mRNA translation.

Cell to cell permeability changes by CAR expression levels in HepG2 cells

In vitro experiments were performed using HepG2 cells. Proteins were extracted and subjected to western blot analysis at 72 h after siCAR transfection. APOBEC3C, ApoB, and LDLR expression increased in CAR-silenced HepG2 cells in a time-dependent manner (Fig. 3A,B). We investigated whether lipid accumulation increased due to the silencing of CAR under transient conditions using siCAR delivery. When CAR was silenced, lipid uptake significantly increased compared to the scrambled siRNA-transfected control (Fig. 3C). In addition, we

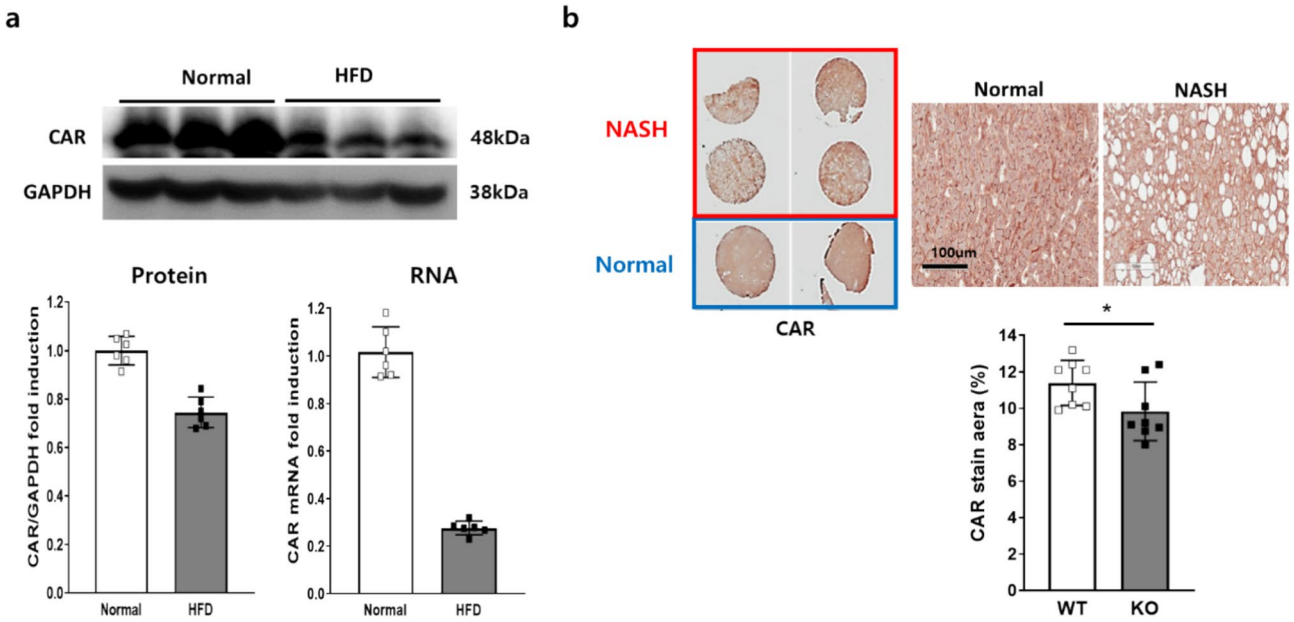

Fig. 1. CAR expression decreases in obese mice and liver samples of patients with NASH. Total RNA and protein were extracted from mice livers after a high-fat diet (HFD). (**A**) CAR mRNA expression in the liver of obese mice was significantly decreased ($P < 0.01$; $n = 3$). Total protein was subjected to western blot analysis and then incubated with anti-CAR antibodies. CAR protein expression level was decreased ($P < 0.05$; $n = 3$). (**B**) The liver tissue Histo-dot of patients with NASH was subjected to immunohistochemistry and then incubated with anti-CAR antibodies. Liver cell–cell junction CAR expression levels were decreased in liver specimens of patients with NASH. Data are expressed as mean ± SD, $^{*}P < 0.05$; $^{**}P < 0.01$.

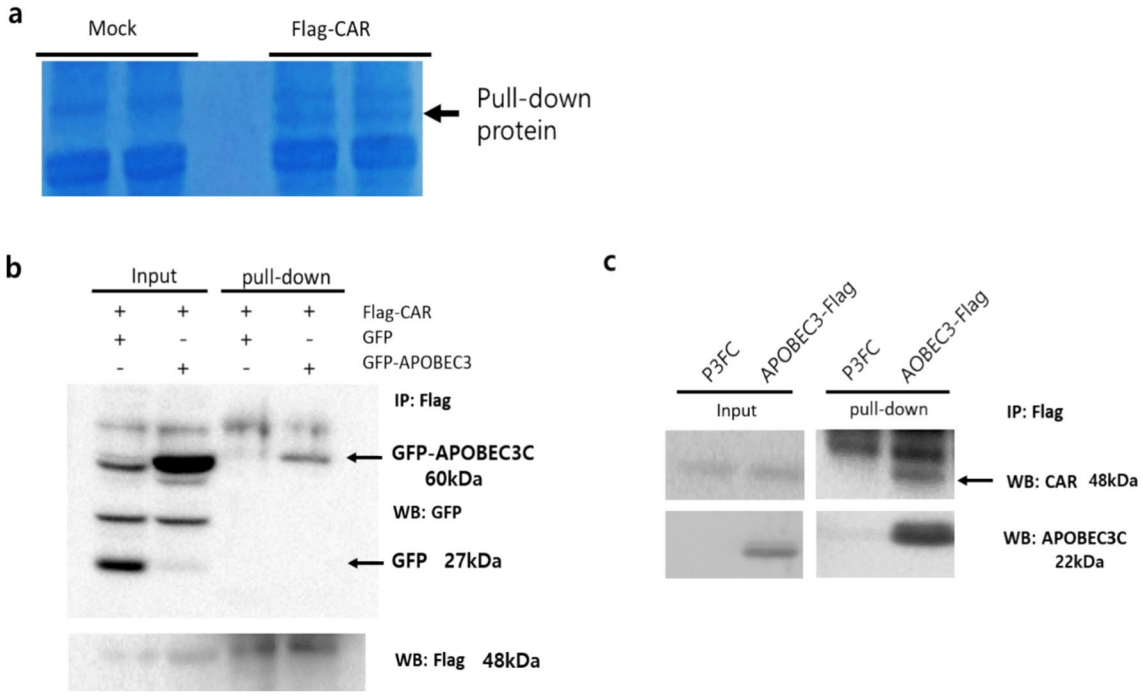

Fig. 2. CAR interacts with a new partner, APOBEC3C. (**A**) FLAG-CAR was overexpressed and pulled down by anti-FLAG agarose to find an interaction partner. The pull-down protein band was sliced and subjected to mass spectrometry. A new interaction protein, APOBEC3C, was identified. (**B**) These two protein interactions were confirmed by co-immunoprecipitation after overexpression of FLAG-CAR and GFP-APOBEC3C. Total protein was extracted and subsequently pulled down by anti-FLAG agarose. Agarose binding protein was subjected to western blot analysis using anti-GFP antibodies. (**C**) The opposite experiment was also performed after APOBEC3C-FLAG overexpression. FLAG agarose pull-down precipitated intracellular proteins were subjected to western blot analysis using anti-CAR antibodies.

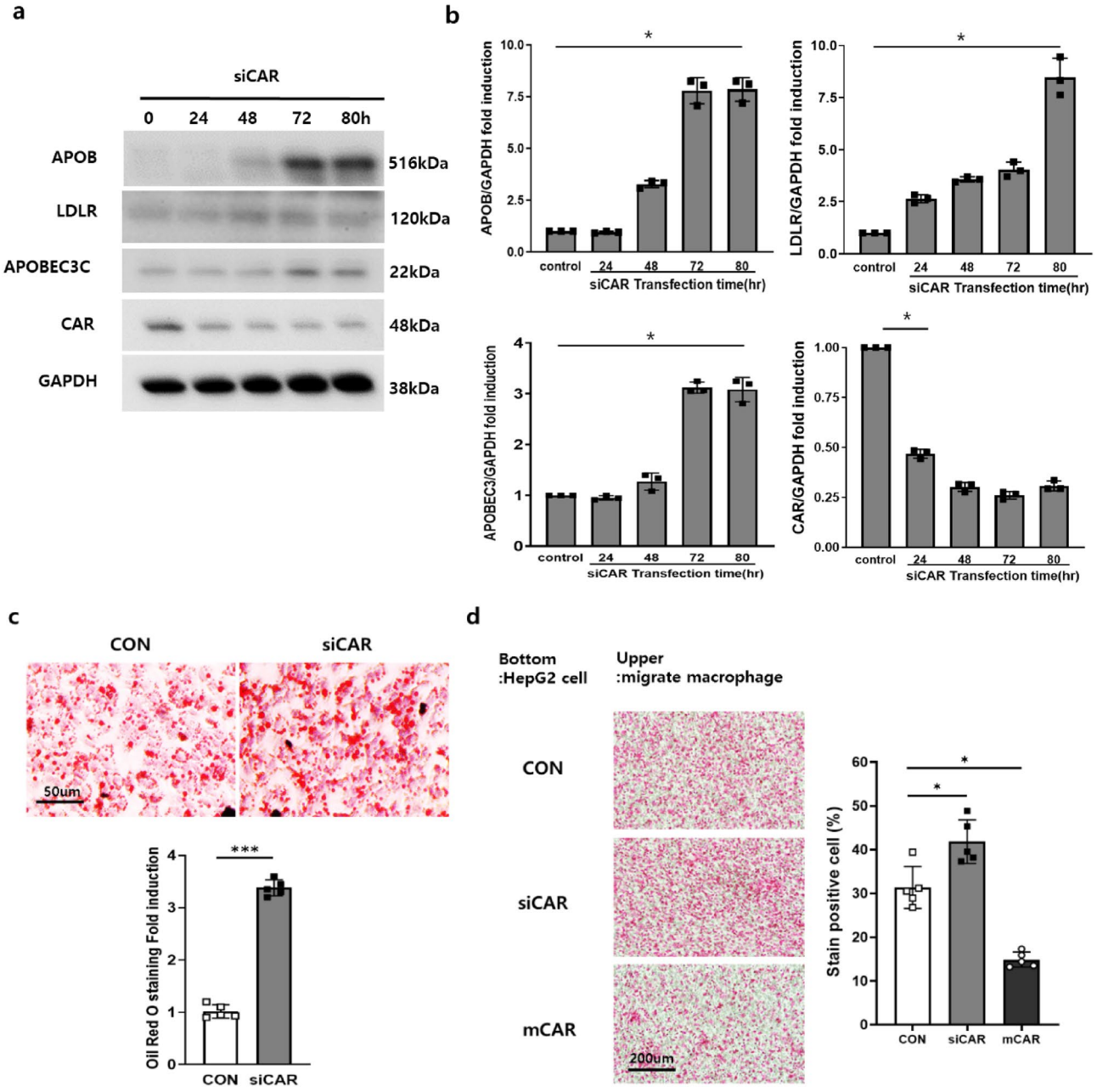

Fig. 3. Transient CAR deletion increases lipid transport regulatory protein and macrophage migration. (**A**,**B**) HepG2 cells were transfected with siCAR and scramble RNA as control (Con). Oleic acid treatment and Oil Red O staining were performed to determine lipid uptake levels in CAR deletions. At various time points (24, 48, 72, and 80 h) after siCAR delivery, cellular proteins were extracted and subjected to western blot analysis using anti-ApoB, -LDLR, -APOBEC3C, -CAR, and -GAPDH antibodies. (**C**) HepG2 cell lipid uptake was investigated by Oil red O staining after siRNA delivery. (**D**) Transwell chamber macrophage migration assay was performed after siCAR (for deletion) or mouse CAR (mCAR; for overexpression) transfection into bottom HepG2 cells. The upper chamber transwell passed macrophage was stained by Eosin (pink dot). Data are expressed as mean ± SD, *P < 0.05; **P < 0.01; ***P < 0.001.

performed a macrophage migration assay using a transwell chamber to identify additional causes of intracellular inflammatory cell infiltration into the livers of CAR-deficient mice. Macrophage migration into CAR-overexpressing HepG2 cells was approximately 50% lower than that into empty plasmid-transfected control cells. In contrast, CAR deletion dramatically increased macrophage migration (Fig. 3D). The macrophage migration assay showed that CAR expression plays an indirect role in the paracellular permeability of macrophages. Cellular studies have shown that reduced CAR protein expression in hepatocytes has a significant effect on lipid accumulation and cell-to-cell permeability.

Generation of liver-specific conditional CAR knockout (KO) mice and liver protein expression

To determine whether CAR expression in the liver cell–cell junction is important for regulating lipid import or export, liver-specific CAR KO mice were generated using CAR floxed mice with albumin-Cre transgenic mice (f/f Cre). KO mice were sacrificed at 16 weeks of age with their littermates (f/f) as wild-type (WT) controls. Liver CAR expression was observed using immunofluorescence staining and western blot analysis. KO mice showed CAR deletion in liver hepatocytes compared with WT mice (Fig. 4A). APOBEC3C protein expression levels were observed in the livers of CAR-KO mice using western blot analysis. APOBEC3C and LDLR protein levels were significantly increased in the livers of CAR KO mice compared to WT mice fed a normal chow diet. This was the only result of CAR disruption phenotype. CAR stability may be related to liver lipid storage regulation systems. APOBEC3C expression was approximately two-fold higher in the livers of CAR-deficient mice than in those of WT mice (Fig. 4B, n = 4). In addition, we isolated hepatocytes from WT and KO mice livers to confirm whether CAR deletion directly regulates hepatocyte lipid absorption and related gene expression. Oil Red O staining showed significantly increased lipid uptake in CAR-deleted hepatocytes compared to WT hepatocytes. APOBEC3C, ApoB, and LDLR mRNA expression was also increased in CAR KO mouse hepatocytes, which was similar to the liver extract protein (Fig. 4C and 4D).

These results show that the CAR intermediate APOBEC3C can regulate ApoB and LDLR expression in the mouse liver. CAR disruption upregulates lipid permeability in the liver and cholesterol absorption in hepatocytes. This can lead to fatty liver disease in the absence of alcohol.

Hepatic lipid droplets and inflammatory cell infiltration are induced by HFD in liver-specific CAR-KO mice

Despite the effective reduction in CAR levels in the livers of CAR KO mice, there was no difference in body and liver weights compared to those of WT mice in pair-fed and HFD mice. During pair-feeding, the KO mice showed no phenotype (Fig. 5A,B, n = 4). We observed a relationship between CAR expression in hepatocytes and the induction of fatty liver disease after 16 weeks of HFD feed. The body weight of KO mice significantly increased at 15 and 16 weeks compared to that of WT mice (Fig. 5A, n = 4). Moreover, HFD-fed mice showed dramatic liver damage in CAR KO mice compared to WT mice. ALT (91 ± 8 vs. 149 ± 18 IU/L) and AST (162 ± 12 vs. 225 ± 9, WT vs. KO) increased due to HFD. In addition, serum triglyceride (TG, 117 ± 28 vs. 236 ± 47 mg/dL) level was significantly increased in KO mice, but serum total cholesterol level (194 ± 37 vs. 270 ± 73 mg/dL) was not different between them (Fig. 5B). H&E and lipid-Tox staining revealed liver lipid droplets and inflammatory cell infiltration. Interestingly, the livers of CAR KO mice showed increased inflammatory cell infiltration and lipid droplets (red) compared to those of WT mice (Fig. 5C,D, and Supplementary Table 3). In addition, peritoneal fat size dramatically increased in CAR KO mice. These data suggest that CAR deletion can affect the regulation of liver lipid permeability and storage. It dramatically changes fat accumulation in the peritoneal cavity.

Liver cholesterol and macrophage infiltration are induced by HFD in liver-specific *CAR* KO mice

After CAR deletion in mouse liver, the livers were analyzed by ELISA to identify total cholesterol, triglyceride, and LDL cholesterol levels. A significant increase in liver total and LDL cholesterol levels was observed in CAR KO mice than in WT mice fed an HFD. However, no difference was observed in pair-fed mice (Fig. 6A, n = 4). CAR disruption increases liver cell-to-cell permeability and may affect liver cholesterol storage regulation and inflammatory cell infiltration. Hepatocyte CAR silencing may cause NAFLD. We identified the relevant genes by qPCR to investigate induced ApoB, APOBEC3C (Fig. 6B), and cytokine (IL-1β, IL-6, TNF-α, and monocyte chemoattractant protein-1 [MCP-1]) changes by increased inflammation in the liver of CAR KO mice. Inflammatory cytokines (IL-1β, IL-6, and TNF-α,), especially MCP-1, were significantly increased in KO mice fed an HFD. No difference in cytokine mRNA expression was observed between the pair-fed mice (Fig. 6C). Liver macrophage infiltration was confirmed by F4/80 IFA staining and mRNA qPCR. Macrophage infiltration was significantly increased due to HFD in CAR KO mice compared to WT mice (Fig. 6D). These data imply that liver-specific CAR deficiency induces MAFLD owing to inflammatory cytokine hyperreactivity, immune cell invasion, and lipid accumulation in HFD-induced obesity.

Discussion

CAR located on the cell surface, function as epithelial cell adhesion molecules and contribute to cell-to-cell permeability homeostasis. CAR can enhance inflammatory interactions between immune and muscle cells during cardiac myocyte communication. CAR plays a crucial role in maintaining structural integrity, particularly in cardiac myocytes[9–13,16]. However, the role of CAR in the liver or hepatic lipid metabolism is poorly understood. This study revealed a novel role and interaction partner for CAR in the liver. CAR mRNA and protein expression levels decreased in the livers of obese mice, indicating a relationship between CAR and hepatic lipid accumulation. CAR deletion in the mouse liver significantly increased monocyte numbers. Notably, the absence of CAR in the liver increased the absorption of Evans Blue dye injected into the tail vein. Additionally, CAR KO mice develop MAFLD through an HFD, resulting in increased inflammation and macrophage infiltration. In contrast, hepatocytes overexpressing CAR exhibited reduced macrophage migration. Transfection with CAR siRNA markedly increased fatty acid absorption by hepatocytes. These findings suggest that CAR expression on the cell surface plays a crucial role in cell-to-cell permeability, regulates lipid uptake, and contributes to overall liver function.

Fatty liver arises from metabolic dysregulation stemming from an excess supply of fat and energy that exceeds the adipose tissue storage capacity. This leads to adipocyte accumulation in the liver, triggering increased triglyceride synthesis and the disruption of blood secretion, particularly lipoprotein synthesis. MAFLD development is closely associated with ApoB, a crucial apolipoprotein facilitating the transfer of TGs and cholesterol[1,26,28–30]. Our study revealed a significant link between MAFLD and CAR. Notably, CAR interacts with APOBEC3C,

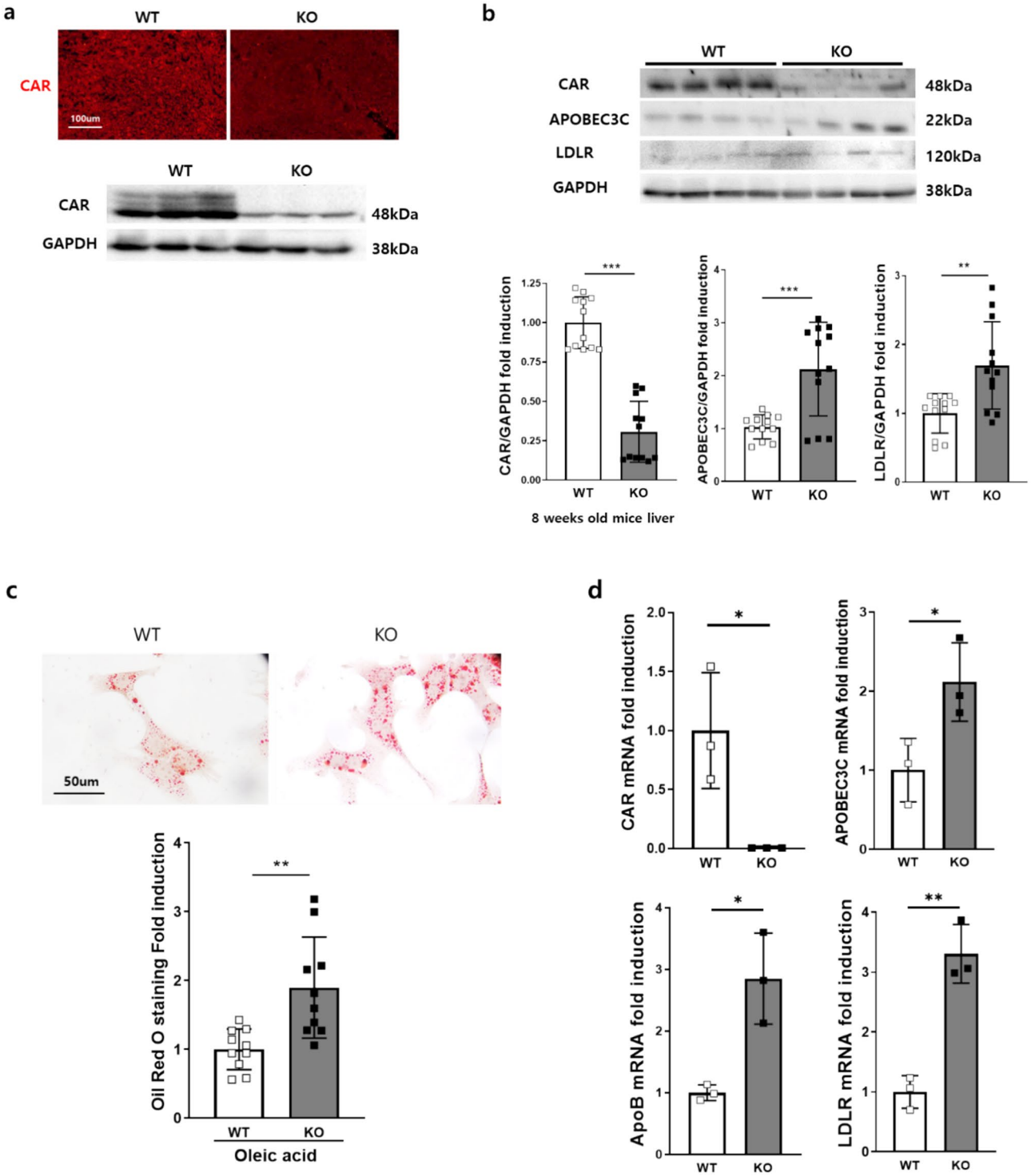

Fig. 4. Generation of liver-specific CAR knockout mice and liver protein expression. (**A**) CAR deletion confirmed liver of 8-weeks-old WT and KO mice by immunofluorescence stain and western blot analysis. (**B**) Protein was extracted from the livers of WT and KO mice and then subjected to western blot analysis using anti-CAR, -APOBEC3C, and -LDLR antibodies (n = 4 for each group). CAR deletion altered lipid transport regulatory proteins and gene expression in the isolated hepatocytes. (**C**) The liver hepatocytes of WT and KO mice were isolated and then subjected to a lipid uptake assay. Oil Red O staining showed lipid uptake levels in the hepatocytes. (**D**) APOBEC3C, ApoB, and LDLR mRNA levels were measured in WT and KO hepatocytes by qPCR. Data are expressed as mean ± SD, *P < 0.05; **P < 0.01; ***P < 0.001.

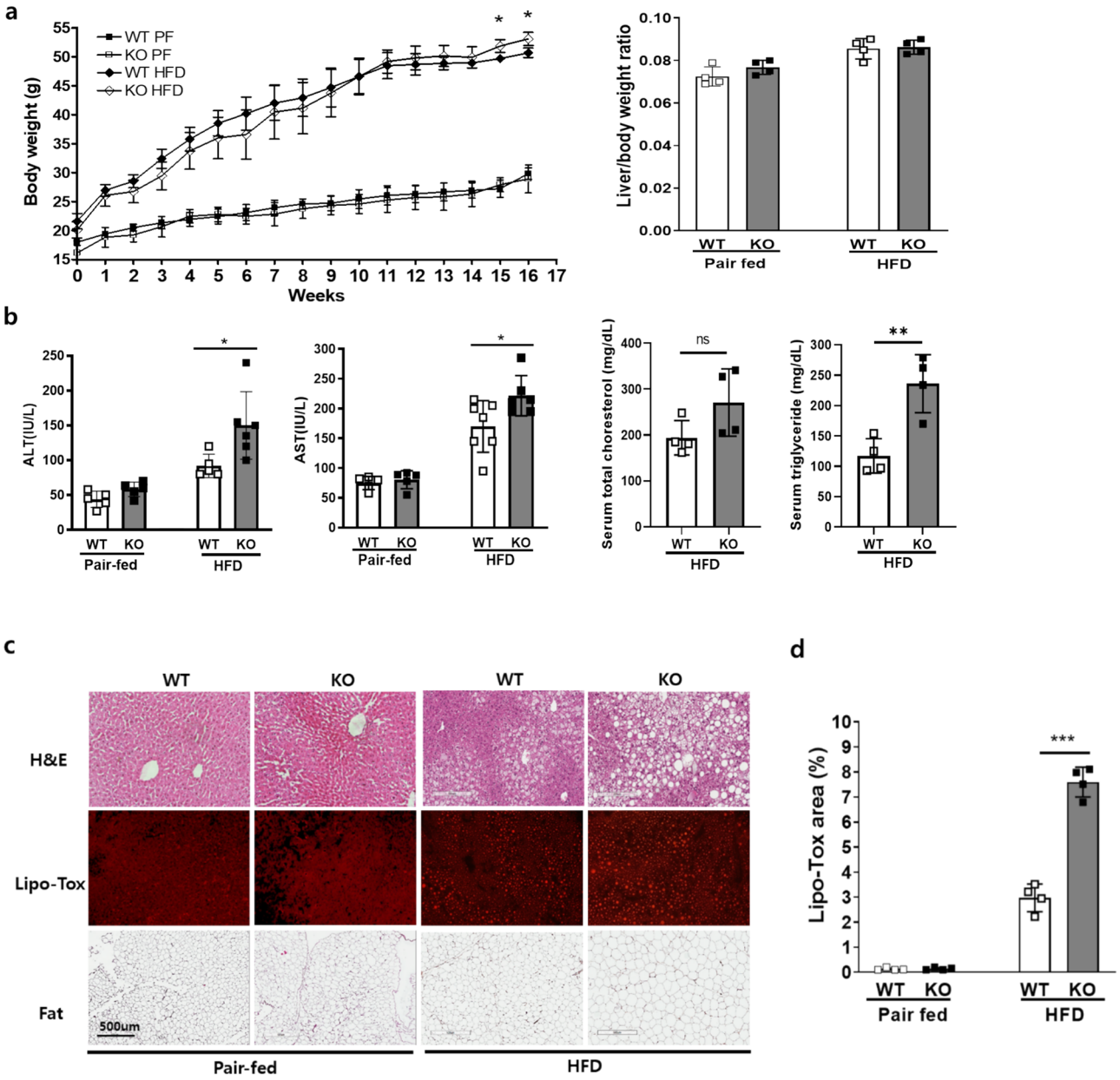

Fig. 5. HFD-induced non-alcoholic fatty liver diseases in liver-specific CAR KO mice. (**A**) The basal phenotype of liver-specific CAR KO mice was confirmed. Body and liver weight were measured under different diet conditions for 16 weeks in pair-fed (■ WT and □ KO) or HFD (◆ WT and ◇ KO) (n = 4 each group) mice. (**B**) Concentrations of ALT, AST, total cholesterol, and triglyceride (TG) in serum were measured using ELISA (n = 4 in each group). (**C**,**D**) After HFD for 16 weeks, the liver was subjected to histological analysis by H&E and neutral lipid Lipo-Tox staining. Peritoneal fat was observed in the paraffin section. Lipid droplets increased in KO mice compared to WT fed an HFD. However, there was no difference between pair-fed mice. Data are expressed as mean ± SD, *P < 0.05 by a two-tailed Student's t-test.

an enzyme that edits ApoB mRNA. In our experiments, overexpressing FLAG-tagged CAR in HEK293 cells and conducting pull-downs with FLAG-agarose identified APOBEC3C as a novel CAR-interacting partner. Subsequent experiments involving the co-transfection of FLAG-CAR with GFP-hAPOBEC3C confirmed their interaction using FLAG-agarose pull-down.

Surprisingly, removing CAR from the livers of mice resulted in elevated expression levels of APOBEC3C and ApoB. APOBEC3C acts as an intermediary mediator contributing to increased ApoB levels (Supplementary Fig. 2). Furthermore, APOBEC3C plays a role in inhibiting retroviral replication[25,27], although the precise mechanism by which CAR induces APOBEC3C expression remains unknown. Experiments manipulating or inhibiting CAR expression in cellular and in vivo contexts have provided compelling evidence that a CAR-APOBEC3C-ApoB pathway significantly influences hepatic lipid metabolism. This newfound understanding of CAR-related pathways sheds light on potential molecular targets for therapeutic interventions in MAFLD.

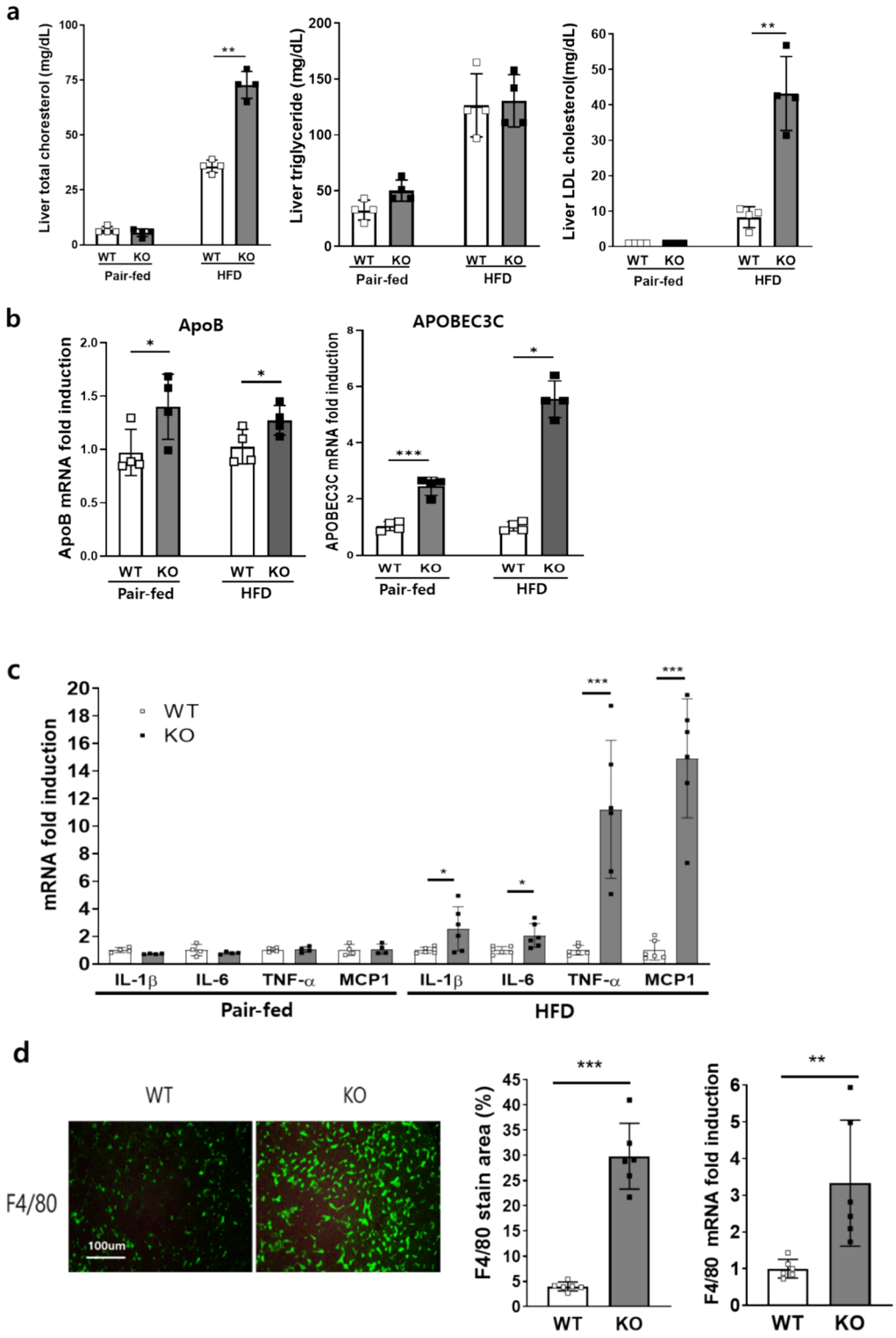

Fig. 6. HFDs induced inflammatory cytokine expression and cholesterol accumulation in the liver of KO mice. (**A**) Liver protein was extracted and then subjected to ELISA. The total cholesterol, triglyceride, and LDL cholesterol levels were measured. (**B**) Total RNA was extracted from mice liver after being pair-fed or fed an HFD and then subjected to qPCR analysis of ApoB and APOBEC3C. In addition, (**C**) inflammatory cytokines (IL-1β, IL-6, TNF-α, and MCP-1) and immunocytes (F4/80: macrophage marker; n = 4). (**D**) Liver subjected to immunofluorescent stain for macrophages. Liver samples were incubated with anti-F4/80 antibodies and Alexa488-labeled secondary antibodies. Infiltrated macrophages presented are by green stain percent area. Data are expressed as mean ± SD, *P < 0.05; **P < 0.01; ***P < 0.001 by a two-tailed Student's t-test. *IL-1β* interleukin-1 beta; IL-6, interleukin-6; *TNF-α* tumor necrosis factor alpha, *MCP-1* monocyte chemoattractant protein-1.

Numerous studies are underway to target and improve steatosis, which is a key factor in the development of this disease. Previous studies have indicated the association of β-catenin with adipocyte formation and steatosis. The WNT/β-catenin pathway is crucial for maintaining vascular permeability and TJs[31–33]. In our previous study, we reported that CAR interacts with β-catenin through its intracellular domain. Recent studies have highlighted the diverse roles of CAR in various cell types, including features such as epithelial permeability, cellular migration, neurite outgrowth, and immune response. Given the interaction of CAR with numerous signaling molecules through its intracellular domains, there is a growing understanding that the regulation of CAR expression significantly affects cell homeostasis[9,13,20,21]. Recently, THRβ agonist has been approved as a drug for MAFLD through the FDA. Thyroid hormones (THs) are essential regulatory molecules for normal growth and development, and for maintaining metabolic homeostasis. Most of the activities elicited by THs are mediated by nuclear thyroid hormone receptors (THRs). THRβ agonist may directly regulate hepatic carbohydrate and lipid metabolism and activate fat use. It also helps to reduce fat accumulation in chronic liver diseases[34,35]. This therapeutic way is a hormonal signal regulation. It possibly has even weak cytotoxicity or some side effects on another organ. Coxsackievirus and adenovirus receptor (CAR) are different types of therapeutic targets. Aging will increase cell-to-cell mechanical permeability and change molecule accumulation such as lipids. The maintenance of CAR may help preserve hepatic permeability and metabolism change due to high lipid accumulation.

This study aimed to explore the relationship between CAR and MAFLD. To observe the decrease in CAR expression in the livers of obese mice, we generated liver-specific CAR KO mice to investigate its role in liver lipid accumulation. Although no specific phenotype was observed in CAR KO mice compared to controls, 16-week HFD resulted in increased macrophages, inflammatory cytokines, and liver cell-to-cell permeability. Elevated MCP-1 levels, which are associated with lipid accumulation and significant in monocyte and macrophage recruitment, were observed[36]. Post-HFD fatty liver induction is believed to involve increased macrophage uptake and cytokine hypersecretion. APOBEC3C upregulation activates the RAS/MAPK signaling pathway and promotes tumor progression[37,38]. However, we still don't know the relation between APOBEC3C and macrophage recruitment. We need to focus more on the APOBEC3C direct role related to macrophages; this should be very interesting research. CAR was removed to study fat transport within hepatocytes, CAR deletion revealed increased lipid accumulation. This suggests that CAR influences hepatocyte cell-to-cell permeability and lipid transport. Additionally, an interaction between CAR and APOBEC3C was identified, with CAR removal leading to increased APOBEC3C levels and the subsequent elevation of ApoB levels. Previous studies have shown that ApoB expression is regulated by an ApoB-editing enzyme, implying that increased ApoB levels may contribute to fatty liver development[26].

In conclusion, our findings highlight the crucial role of CAR in hepatocyte cell-to-cell permeability, correlating APOBEC3C and ApoB as part of a significant pathway for fat accumulation. Targeting CAR can be a potentially effective strategy for treating MAFLD.

Methods

Animals and experimental design

All animal models shown were on C57BL/6 background mice. To identify the role of CAR in the liver, we generated liver-specific conditional CAR knock-out mice (CAR-KO)[9]. All experiments were performed in accordance with the relevant guidelines and regulations. For CAR-KO mice, a floxed CAR construct was generated by inserting loxP sites just before and after the second exon, as we reported previously, and mated Albumin-Cre mice. Mice were fed for 16 weeks either normal chow (3.5% fat) or a high-fat diet (HFD) (42% fat, 0.2% cholesterol) and had free access to water. After 16 weeks of HFD treatment, the mice were euthanized by CO_2 inhalation, and their livers and serums were harvested for further analysis. All animal experiments used four-week-old CAR-KO (f/f Cre) mice and their littermate wild-type (f/f or f/ + without Cre, WT) male mice (about 18 g in weight). Cardiac-specific CAR KO mice housing on the animal facility. The dimmers were used in mouse rooms to create twilight periods between the light and dark cycles. A room temperature between 20–26 °C was maintained. All procedures were complied with the ARRIVE guidelines and approved by the Institutional Animal Care and Use Committee of the Samsung Biomedical Research Institute (#20200518001). SBRI is accredited by the Association for Assessment and Accreditation of Laboratory Animal Care International (AAALAC International) and abides by the Institute of Laboratory Animal Resources (ILAR) guide.

Preparation of expression plasmids

The full-length human or mouse CAR gene was amplified by polymerase chain reaction (PCR) from human heart cDNA or C57BL/6 mouse heart cDNA, respectively. Human CAR or mouse CAR was cloned into the p3xFlag-CMV-10 (Sigma-Aldrich, MO, USA) vector. The full-length human APOBEC3C gene was amplified by PCR from the HEK293 cell. Human APOBEC3C was cloned into the pEGFP-C3 (Clontech, CA, USA) vector. The expression vector was applied for full-down assay.

Cell culture and transfection

HEK293 or HepG2 cell lines were cultured in DMEM or RPMI containing 10% fetal bovine serum (FBS) and 1% penicillin/streptomycin solutions. Cells were transfected with 1ug expression plasmids using 1 mg/ml polyethyleneimine (PEI) (Sigma-Aldrich, MO, USA) for 24 h. The DNA and PEI mixture is based on a 5:1 ratio of PEI (ug): plasmid DNA (ug) and incubated for 15 min at RT. All expression plasmid experiments were transfected with each gene cloned with empty plasmids as controls.

Reverse transcription and quantitative real-time PCR

Total RNA was isolated from mouse liver using the easy-spin™ Total RNA Extraction Kit (iNtRON, Seongnam, KOR). Reverse transcription (RT) was performed using ReverTraAce qPCR RT Kit (TOYOBO, Osaka, JAP). Quantitative real-time PCR (qPCR) was performed using the NEXpro™ qPCR Master Mix (SYBR) High Rox (NEX™ Diagnostics, Seongnam, KOR). To compare the mRNA levels of genes associated with inflammation, apolipoproteins, and immune cells. The primer sets used were synthesized by SFC-probe (Cheongju, Korea). The primer sequences are listed in Supplementary Table 1.

Western blot analysis

Protein was extracted from frozen liver samples or cultured cells. Approximately 20 μg of protein was separated on SDS–Polyacrylamide gel (10%) electrophoresis and transferred to PVDF membranes. Western blot analysis was performed by an ECL detection using ChemiDoc XRS + system (BIO-RAD, CA, USA), and band intensities were quantified using ImageJ software 1.45 s (https://imagej.net; NIH, MA, USA). Primary antibodies were proved for CAR, GFP, GAPDH, LDLR (Santa Cruz Biotechnology Inc., CA, USA), APOB, and APOBEC3C (Cell Signaling, Danvers, MA, USA).

Tissue microarray immunohistochemistry

Human liver steatohepatitis commercial tissue microarray slide (Lot No. 2010171) purchased from Sekisui Xeno-Tech (Kansa City, KS, USA). We did not get a piece of personal information about the patient and just applied for research. The paraffin-embedded liver microarray slide was proved with anit-rabbit CAR antibody (Santa Cruz Biotechnology Inc., CA, USA) for 18 h at 4 °C. Immunodetection was performed using a Universal Quick Kit (Vector Laboratories, Burlingame, CA, USA) as described in the manufacturer's instructions. Stained tissue images were taken and processed using a light microscope (Olympus Co., San Jose, CA, USA).

Histology and immunofluorescence assay

For Oil Red O staining, liver tissue was performed using 7-μm frozen section and stained Oil Red O working solution (Sigma-Aldrich, MO, USA) with hematoxylin stain. H&E staining and immunofluorescence assay were performed using 7-μm frozen sections as described previously. Primary antibodies were proved by CAR (Santa Cruz Biotechnology Inc., CA, USA). The target proteins were visualized with the secondary antibodies conjugated with fluorescence (Alexa Fluor 488 and 594, 1:400) (Thermofiher Scientific, CA, USA) and Hoechst nuclear stain.

Blood plasma, liver triglyceride, and cholesterol contents

Liver TG or TC levels were measured using a mouse TG or TC ELISA kit following the manufacturer's manuals (MyBioSource, CA, USA). Concentrations of glucose, BUN, ALT, AST, TG, and TC in serum were determined using discrete-type clinical chemistry automated analyzers (Hitachi, Tokyo, JAP).

Macrophage cell migration and lipid uptake assay

Cell migration assays were performed using a modified Boyden chamber approach (Corning, NY, USA). HepG2 cells in the lower chamber were transfected with mouse CAR or P3FC vector as controls for 48 h. Murine macrophages obtained by peritoneal macrophage isolation were maintained in the upper chamber of another plate without cells in DMEM containing 10% FBS. After the macrophage is cultured for 24 h, the upper chamber is transferred to the lower chamber and incubated for 24 h. Macrophages that had migrated through the membrane were stained using eosin, and the migrated cells were analyzed at × 100 magnification using a microscope or ImageJ software 1.45 s (https://imagej.net; NIH, MA, USA). To examine the hepatocyte cell–cell permeability, Mice were injected with 1% Evans blue dye (EBD) in the tail vein. After an hour, mice were sacrificed, and their livers were collected and lysed in PBS. EBD in liver whole lysate was measured by absorbance at 650 nm.

Immunoprecipitation

To identify the interaction partner of CAR, Flag-tagged CAR protein was expressed in HEK293 cells by transfection. The CAR-Flag was pulled down in 1 ml of HEK293 cell extracts 24 h after transfection using agarose beads conjugated with an anti-Flag (M2) antibody (Sigma-Aldrich, MO, USA). The CAR-Flag protein was specifically eluted from the beads by centrifugation at 13,000 RPM for 10 min. protein was separated on SDS–Polyacrylamide gel (10%) electrophoresis and stained using coomassie blue. We cut interesting protein bands and requested a mass spectrometer to identify pull-downed individual proteins (Matrix Science, MA, USA)[9]. The interaction between CAR and APOBEC3C was observed by co-immunoprecipitation assay; flag-tagged CAR protein and GFP-tagged APOBEC3C were expressed in HEK293 cells by transfection. The CAR-Flag was pulled down in 1 ml of HEK293 cell extracts 24 h after transfection using agarose beads conjugated with an anti-Flag (M2) antibody (Sigma-Aldrich, MO, USA). Precipitated agarose beads were washed 5 times and the CAR-Flag protein was specifically eluted from the beads. CAR binding to APOBEC3C was confirmed using the eluted proteins by western blot analysis with GFP antibody. As a negative control, pEGFP-C3 empty plasmid was expressed with CAR. The immunoprecipitation was performed using anti-Flag agarose beads as described previously.

Statistical analysis

All data were analyzed using GraphPad Prism 9 (GraphPad Software, San Diego, CA, USA) and were presented as the means ± standard deviation (SD). To analyze the statistical significance between the two groups, a Student's t-test was used, and one-way ANOVA was used to analyze the statistical significance between multiple groups.

For the analysis of multiple time points experiments, a two-way ANOVA was used. * $p < 0.05$, ** $p < 0.01$, *** $p < 0.001$ was considered significant.

Data availability

The datasets used and/or analysed during the current study available from the corresponding author on reasonable request.

Received: 25 April 2024; Accepted: 9 September 2024
Published online: 16 September 2024

References

1. Machado, M. V. & Cortez-Pinto, H. Non-alcoholic fatty liver disease: What the clinician needs to know. *World J. Gastroenterol.* **20**, 12956–12980 (2014).
2. Behari, J. *et al.* Liver-specific beta-catenin knockout mice exhibit defective bile acid and cholesterol homeostasis and increased susceptibility to diet-induced steatohepatitis. *Am. J. Pathol.* **176**, 744–753 (2010).
3. Sanyal, A. J. *et al.* Pioglitazone, vitamin E, or placebo for nonalcoholic steatohepatitis. *N. Engl. J. Med.* **362**, 1675–1685 (2010).
4. Day, C. P. & James, O. F. Steatohepatitis: A tale of two "hits"?. *Gastroenterology* **114**, 842–845 (1998).
5. Harrison, S. A., Kadakia, S., Lang, K. A. & Schenker, S. Nonalcoholic steatohepatitis: What we know in the new millennium. *Am. J. Gastroenterol.* **97**, 2714–2724 (2002).
6. Zihni, C., Mills, C., Matter, K. & Balda, M. S. Tight junctions: From simple barriers to multifunctional molecular gates. *Nat. Rev. Mol. Cell Biol.* **17**, 564–580 (2016).
7. Severson, E. A. & Parkos, C. A. Mechanisms of outside-in signaling at the tight junction by junctional adhesion molecule A. *Ann. N. Y. Acad. Sci.* **1165**, 10–18 (2009).
8. Goel, R. *et al.* The proinflammatory phenotype of PECAM-1-deficient mice results in atherogenic diet-induced steatohepatitis. *Am. J. Physiol. Gastrointest. Liver Physiol.* **293**, G1205-1214 (2007).
9. Lim, B. K. *et al.* Coxsackievirus and adenovirus receptor (CAR) mediates atrioventricular-node function and connexin 45 localization in the murine heart. *J. Clin. Invest.* **118**, 2758–2770 (2008).
10. Coyne, C. B. & Bergelson, J. M. CAR: A virus receptor within the tight junction. *Adv. Drug Deliv. Rev.* **57**, 869–882 (2005).
11. Asher, D. R. *et al.* Coxsackievirus and adenovirus receptor is essential for cardiomyocyte development. *Genesis* **42**, 77–85 (2005).
12. Cohen, C. J. *et al.* The coxsackievirus and adenovirus receptor is a transmembrane component of the tight junction. *Proc. Natl. Acad. Sci. U S A* **98**, 15191–15196 (2001).
13. Coyne, C. B., Voelker, T., Pichla, S. L. & Bergelson, J. M. The coxsackievirus and adenovirus receptor interacts with the multi-PDZ domain protein-1 (MUPP-1) within the tight junction. *J. Biol. Chem.* **279**, 48079–48084 (2004).
14. Excoffon, K. J., Hruska-Hageman, A., Klotz, M., Traver, G. L. & Zabner, J. A role for the PDZ-binding domain of the coxsackie B virus and adenovirus receptor (CAR) in cell adhesion and growth. *J. Cell Sci.* **117**, 4401–4409 (2004).
15. Liu, P. *et al.* The tyrosine kinase p56lck is essential in coxsackievirus B3-mediated heart disease. *Nat. Med.* **6**, 429–434 (2000).
16. Ortiz-Zapater, E., Santis, G. & Parsons, M. CAR: A key regulator of adhesion and inflammation. *Int. J. Biochem. Cell Biol.* **89**, 1–5 (2017).
17. Verdino, P., Witherden, D. A., Havran, W. L. & Wilson, I. A. The molecular interaction of CAR and JAML recruits the central cell signal transducer PI3K. *Science* **329**, 1210–1214 (2010).
18. Shetty, P. B. *et al.* Variants in CXADR and F2RL1 are associated with blood pressure and obesity in African-Americans in regions identified through admixture mapping. *J. Hypertens.* **30**, 1970–1976 (2012).
19. Ahrens, M. *et al.* DNA methylation analysis in nonalcoholic fatty liver disease suggests distinct disease-specific and remodeling signatures after bariatric surgery. *Cell Metab.* **18**, 296–302 (2013).
20. Raschperger, E. *et al.* The coxsackie- and adenovirus receptor (CAR) is an in vivo marker for epithelial tight junctions, with a potential role in regulating permeability and tissue homeostasis. *Exp. Cell Res.* **312**, 1566–1580 (2006).
21. Mirza, M. *et al.* Coxsackievirus and adenovirus receptor (CAR) is expressed in male germ cells and forms a complex with the differentiation factor JAM-C in mouse testis. *Exp Cell Res* **312**, 817–830 (2006).
22. Hussain, F. *et al.* CAR modulates E-cadherin dynamics in the presence of adenovirus type 5. *PLoS ONE* **6**, e23056 (2011).
23. Nasuno, A. *et al.* Expression of coxsackievirus and adenovirus receptor in neointima of the rat carotid artery. *Cardiovasc. Pathol.* **13**, 79–84 (2004).
24. Rosenberg, B. R., Hamilton, C. E., Mwangi, M. M., Dewell, S. & Papavasiliou, F. N. Transcriptome-wide sequencing reveals numerous APOBEC1 mRNA-editing targets in transcript 3' UTRs. *Nat. Struct. Mol. Biol.* **18**, 230–236 (2011).
25. Yu, Q. *et al.* APOBEC3B and APOBEC3C are potent inhibitors of simian immunodeficiency virus replication. *J. Biol. Chem.* **279**, 53379–53386 (2004).
26. Ashur-Fabian, O. *et al.* apoB and apobec1, two genes key to lipid metabolism, are transcriptionally regulated by p53. *Cell Cycle* **9**, 3761–3770 (2010).
27. Milewska, A. *et al.* APOBEC3-mediated restriction of RNA virus replication. *Sci. Rep.* **8**, 5960 (2018).
28. Riquelme, A. *et al.* Non-alcoholic fatty liver disease and its association with obesity, insulin resistance and increased serum levels of C-reactive protein in Hispanics. *Liver Int.* **29**, 82–88 (2009).
29. Genest, J. Jr. *et al.* Lipoprotein cholesterol, apolipoprotein A-I and B and lipoprotein (a) abnormalities in men with premature coronary artery disease. *J. Am. Coll. Cardiol.* **19**, 792–802 (1992).
30. Wilfred de Alwis, N. M. & Day, C. P. Genes and nonalcoholic fatty liver disease. *Curr. Diabetes Rep.* **8**, 156–163 (2008).
31. Liu, S. *et al.* beta-catenin is essential for ethanol metabolism and protection against alcohol-mediated liver steatosis in mice. *Hepatology* **55**, 931–940 (2012).
32. Song, X. *et al.* Wogonin influences vascular permeability via Wnt/beta-catenin pathway. *Mol. Carcinog.* **54**, 501–512 (2002).
33. Ross, S. E. *et al.* Inhibition of adipogenesis by Wnt signaling. *Science* **289**, 950–953 (2000).
34. Yen, P. M. Physiological and molecular basis of thyroid hormone action. *Physiol. Rev.* **81**, 1097–1142 (2001).
35. Caddeo, A. *et al.* TG68, a novel thyroid hormone Receptor-beta agonist for the treatment of NAFLD. *Int. J. Mol. Sci.* **22**, 1305 (2021).
36. Kanda, H. *et al.* MCP-1 contributes to macrophage infiltration into adipose tissue, insulin resistance, and hepatic steatosis in obesity. *J. Clin. Invest.* **116**, 1494–1505 (2006).
37. Esnault, C. *et al.* APOBEC3G cytidine deaminase inhibits retrotransposition of endogenous retroviruses. *Nature* **433**, 430–433 (2005).
38. Bhattacharya, C., Aggarwal, S., Kumar, M., Ali, A. & Matin, A. Mouse apolipoprotein B editing complex 3 (APOBEC3) is expressed in germ cells and interacts with dead-end (DND1). *PLoS ONE* **3**, e2315 (2008).

Acknowledgements
This study was supported by a grant from the Ministry of Food and Drug Safety (No. 22203MFDS403-1, B.K.L), and the grant of the National Research Foundation (NRF) of Korea provided by the Korean Government (No. NRF-2022R1F1A1063986, B.K.L).

Author contributions
E.-S.J., B.-K.L. conceived and supervised the study. H.-E.J., J.-H.P., H.-H.S, and H.-G.K. contributed to the planning of the animal experiment. H.-E.J., J.-H.P., H.-H.S, H.-G.K., and J.-H.S., performed animal experiments. Y.-S.W., and H.-J.K. performed isolation of hepatocytes. J.-H.P. designed the figure. J.-H.P., E.-S.J., Y.-S.W., and B.-K.L. contributed to manuscript writing.

Competing interests
The authors declare no competing interests.

Additional information
Supplementary Information The online version contains supplementary material available at https://doi.org/10.1038/s41598-024-72561-2.

Correspondence and requests for materials should be addressed to B.-K.L.

Reprints and permissions information is available at www.nature.com/reprints.

Publisher's note Springer Nature remains neutral with regard to jurisdictional claims in published maps and institutional affiliations.

Open Access This article is licensed under a Creative Commons Attribution-NonCommercial-NoDerivatives 4.0 International License, which permits any non-commercial use, sharing, distribution and reproduction in any medium or format, as long as you give appropriate credit to the original author(s) and the source, provide a link to the Creative Commons licence, and indicate if you modified the licensed material. You do not have permission under this licence to share adapted material derived from this article or parts of it. The images or other third party material in this article are included in the article's Creative Commons licence, unless indicated otherwise in a credit line to the material. If material is not included in the article's Creative Commons licence and your intended use is not permitted by statutory regulation or exceeds the permitted use, you will need to obtain permission directly from the copyright holder. To view a copy of this licence, visit http://creativecommons.org/licenses/by-nc-nd/4.0/.

© The Author(s) 2024